Published in final edited form as:

Sci Immunol. 2021 June 04; 6(60): . doi:10.1126/sciimmunol.abg1101.

Abcc1 and Ggt5 support lymphocyte guidance through export and catabolism of S-geranylgeranyl-L-glutathione

Antonia E. Gallman[1,2,3], **Finn D. Wolfreys**[1,2,*], **David N. Nguyen**[4,5], **Moriah Sandy**[1,2], **Ying Xu**[1,2], **Jinping An**[1,2], **Zhongmei Li**[4,5], **Alexander Marson**[4,5], **Erick Lu**[1,2,†], **Jason G. Cyster**[1,2,*]

[1]Howard Hughes Medical Institute, University of California, San Francisco, San Francisco, CA 94143.

[2]Department of Microbiology and Immunology, University of California, San Francisco, San Francisco, CA 94143.

[3]Medical Scientist Training Program, University of California, San Francisco, San Francisco, CA 94143.

[4]J. David Gladstone Institutes, San Francisco, CA 94158.

[5]Department of Medicine, University of California, San Francisco, San Francisco, CA 94143.

Abstract

P2RY8 promotes the confinement and growth regulation of germinal center (GC) B cells and loss of human P2RY8 is associated with B cell lymphomagenesis. The metabolite S-geranylgeranyl-L-glutathione (GGG) is a P2RY8 ligand. The mechanisms controlling GGG distribution are poorly understood. Here, we show that gamma-glutamyltransferase-5 (Ggt5) expression in stromal cells was required for GGG catabolism and confinement of P2RY8-expressing cells to GCs. We identified the ATP-binding cassette, sub-family C member-1 (Abcc1) as a GGG transporter and showed that Abcc1 expression by hematopoietic cells was necessary for P2RY8-mediated GC confinement. Furthermore, we discovered that P2RY8 and GGG negatively regulated trafficking of B and T cells to the bone marrow (BM). Importantly, P2RY8 loss-of-function human T cells increased their BM homing. By defining how GGG distribution was determined and identifying sites of P2RY8 activity, this work helps establish how disruptions in P2RY8 function contribute to lymphomagenesis and other disease states.

One Sentence Summary:

This work establishes how P2RY8 ligand is exported and degraded to regulate lymphocyte behavior in lymphoid follicles and bone marrow.

[*]Corresponding authors: Jason G Cyster (Jason.Cyster@ucsf.edu) and Finn D Wolfreys (Finn.Wolfreys@ucsf.edu).
[†]Current address: TRex Bio, South San Francisco, CA 94080

Author contributions: A.E.G. designed and performed experiments, interpreted the results, and wrote the manuscript. F.D.W. provided intellectual input, designed experiments, helped with LC-MS/MS and synthesized GGG. E.L. provided intellectual input and performed MK571 experiments. D.N.N. provided intellectual input and edited human T cells. M.S. provided intellectual input and performed LC-MS/MS measurements. Y.X., J.A., and Z.L. generated and screened knockout mice and performed PCR analysis. A.M. supervised the CRISPR experiments. J.G.C. designed experiments, interpreted results, supervised research and wrote the manuscript.

Competing interests: The authors declare no competing interests.

Introduction

P2RY8 is a G-protein coupled receptor (GPCR) that is frequently mutated in GC B cell-derived diffuse large B cell lymphoma (GCB-DLBCL) and Burkitt lymphoma (BL) (1–6). Loss of receptor function contributes to both dissemination and growth deregulation in lymphoma cells (1). P2RY8 is highly expressed by GC B cells and T follicular helper (Tfh) cells. Downstream signaling through P2RY8 via Gα13-containing heterotrimeric G-proteins promotes confinement of B cells in the follicle center (1). However, P2RY8 is also expressed more broadly in human lymphocytes and some other immune cell types, suggesting functions beyond the GC. Gα13 in lymphocytes activates ArhGEF1 to then activate Rho and inhibit cell migration towards chemoattractants (7). This signaling pathway also suppresses AKT activation, and P2RY8 can exert a growth repressive effect on GC B cells. While widely conserved in vertebrates, P2RY8 lacks a sequence ortholog in rodents (1). However, it has been possible to study P2RY8 function by placing the human receptor in mouse cells and transferring the cells into mice; such work established the confinement and growth regulatory activities of P2RY8 (1, 8). By helping confine GC B cells and Tfh cells to individual GCs, P2RY8 may foster unique paths of B cell clonal evolution in separate GCs, thereby contributing to the overall diversity of the antibody response(9).

The metabolite, S-geranylgeranyl-L-glutathione (GGG) was identified using classical biochemical fractionation approaches as a nanomolar potent ligand for P2RY8 in a migration inhibition assay (7). Human tonsil, mouse spleen, and mouse lymph node (LN) extracts contain low nanomolar concentrations of GGG, indicating that it is present in lymphoid tissues at levels shown to be active on the receptor *in vitro*. GGG is also abundant in liver tissue and bile and produced by many cell lines (7). When mixed with chemokines, GGG inhibits migration of $P2RY8^{+}$ cells towards the chemokine (7). The actions of P2RY8 as a GC confinement factor that inhibits the migration of GC B cells towards chemokines has led to a model in which GGG is more abundant in the outer regions of lymphoid follicles and less abundant at the follicle center (10). To understand how GGG is distributed in tissues it is necessary to determine the enzymes involved in GGG metabolism and transport, as well as how it is exported by cells.

Glutathione conjugated lipids are often catabolized by gamma-glutamyl transferases (Ggt), peptidase-like enzymes that cleave the gamma-glutamyl bond in the glutathione tripeptide to generate CysGly + Glu (11). Expression of the 5 Ggt family members in HEK293T cells has demonstrated that Ggt5 is most active towards GGG, converting it into GG-CysGly and Glu, with Ggt1 and Ggt2 demonstrating weak activity (7). Ggt5 is highly expressed by human and mouse follicular dendritic cells (FDCs), stromal cells located in the center of lymphoid follicles, supporting the idea that it may be a key enzyme in GGG catabolism in lymphoid tissues (7). Moreover, overexpression of Ggt5 in follicular B cells *in vivo* is sufficient to disrupt the confinement-promoting function of P2RY8 (7). However, whether Ggt5 is necessary for establishing P2RY8-guiding GGG gradients *in vivo* has not been determined.

As a conjugate of glutathione, GGG likely requires export from the cytoplasm via a specific transporter, given this requirement for all previously described glutathione conjugates (12). Of the 48 ATP-binding cassette (ABC) transporters, the 12-member ABCC subfamily includes proteins specialized for efflux of glutathione-conjugated molecules (12). In particular, ABCC1 (MRP1) transports leukotriene-C4 (LTC4), oxidized glutathione (GSSG) and a range of GSH-drug conjugates (12). Several other family members can also transport glutathione conjugated drugs and metabolites (13). Whether any of these transporters are involved in GGG export by cells and the establishment of interstitial GGG gradients is unknown.

In this study we demonstrated that Ggt5 was important for catabolism of GGG, and expression of this enzyme by stromal cells was necessary for maintaining the GGG distribution that supports P2RY8-mediated confinement of cells. We identified Abcc1 as a GGG transporter and showed that it functioned in both hematopoietic and non-hematopoietic cells to allow their production of the extracellular GGG, which was needed for P2RY8 organizing functions. Abcc1 was also required for P2RY8 inhibition of GC B cell expansion, most notably in the Peyer's Patches (PP). Finally, we demonstrated that P2RY8 and GGG restrained lymphocyte homing to the BM. This work defines key molecular and cellular requirements for establishing GGG distribution within tissues and shows that P2RY8 influences cell behavior within BM as well as secondary lymphoid organs.

Results

Ggt5 was necessary for lymphoid tissue GGG catabolism:

To determine the contribution of Ggt5 to the *in vivo* regulation of GGG distribution we used CRISPR/Cas9 to generate mice deficient in this enzyme (Supplementary Fig. 1A,B). The mice were engineered to harbor an exon 1 deletion analogous to that previously shown to disrupt Ggt5 leukotrienase function in mice (14). GGG abundance was measured in bile fluid and in spleen extracts from control and Ggt5 null mice using LC-MS/MS (Fig. 1A.B). GGG is present in high amounts in bile (7) and was increased approximately two-fold upon Ggt5 deficiency (Fig. 1A). Importantly, splenic GGG increased more than eight-fold in Ggt5-deficient mice (Fig. 1B). These data established that Ggt5 was critical *in vivo* for GGG catabolism, especially within lymphoid tissue.

We next tested whether Ggt5 was required for P2RY8-mediated confinement of B cells to the GC. We hypothesized that loss of Ggt5 would disrupt the established GGG gradient throughout the follicle, eliminating regions of low GGG maintained by active degradation. This alteration would be expected to compromise the ability of P2RY8 to confine cells to the GC, as the GC would no longer be a local minimum of GGG concentration (10). B cells retrovirally transduced to express P2RY8 (Supplementary Fig. 1C,D) were transferred into either pre-immunized Ggt5-deficient or wildtype control mice and were examined for their localization in the spleen one day later. While empty vector (EV)-transduced control cells were found throughout the IgD^+ region of the follicle, P2RY8 expressing cells clustered tightly over the FDC-rich region of the GC of wildtype mice as expected (Fig. 1C and Supplementary Fig. 2A). In contrast, when $P2RY8^+$ cells were transferred into Ggt5-deficient mice, the cells failed to cluster in the GC (Fig. 1C and Supplementary Fig.

2A). A loss of P2RY8$^+$ cell confinement in GCs was also seen in the mLNs (Supplementary Fig. 2B). Additionally, the confinement of P2RY8$^+$ cells to the FDC network in the center of primary follicles of unimmunized mice was also Ggt5-dependent (Supplementary Fig. 2C). These data provided strong evidence that Ggt5-mediated catabolism of GGG is required for P2RY8 function in guiding B cell distribution within follicles across multiple lymphoid tissues and immunization states.

Ggt5 degrades leukotriene C4 (LTC4), a glutathione-conjugated lipid that acts as an intercellular signaling molecule (15, 16). LTC4 has two well established high affinity receptors (CysLTR1 and CysLTR2) (17). Using a bioassay with nanomolar sensitivity we previously observed *in vitro* that LTC4 also has activity on P2RY8, though with a 100-fold less potency than GGG (7). To exclude the possibility that the lack of P2RY8$^+$ cell clustering identified in Ggt5-deficient mice was due to an effect on LTC4 rather than GGG, we performed transfers of P2RY8$^+$ cells into mice deficient in arachidonate 5-lipoxygenase, or 5-LO, which lack the ability to generate LTC4 (18). P2RY8$^+$ cells transferred into pre-immunized 5-LO-deficient mice continued to cluster over the FDC network in the GC (Supplementary Fig. 2D) excluding a role for LTC4 in this process.

Ggt5 is expressed highly by FDCs in both human tonsil and mouse lymphoid tissues (7). To determine if expression of Ggt5 was required in the stromal compartment for the clustering of P2RY8$^+$ cells, we generated chimeric mice in which Ggt5 sufficient or deficient BM was transferred into Ggt5 sufficient or deficient irradiated hosts and the mice were allowed to reconstitute. Transferred P2RY8$^+$ B cells failed to cluster in the splenic and lymph node GC of mice lacking Ggt5 in the radioresistant, stromal compartment, but not in mice lacking Ggt5 in the hematopoietic compartment (Fig 1D and Supplementary Fig 2E). These data supported a model in which Ggt5 expression by radioresistant FDCs *in vivo* acts to degrade local GGG, allowing for the confinement of P2RY8 expressing cells to the GC.

Abcc1 was a GGG transporter:

Owing to glutathione's polarity, glutathione conjugates generally rely on active transport, rather than passive diffusion, to leave cells. Other glutathione conjugated molecules are transported by members of the Abcc family (12). Of the family's 11 members, Abcc1, Abcc4, Abcc5, and Abcc9 are highly expressed in mouse lymphoid tissue (Supplementary Fig 3A). GGG is produced by several human cell lines, including HEK293T cells (7), which express high levels of Abcc1, Abcc4, Abcc5, and Abcc10 (Supplementary Fig 3B). MK-571 is an inhibitor of Abcc1, though with low specificity (19). When HEK293T cells were cultured in the presence of MK-571, the ability of the culture supernatants to inhibit P2RY8$^+$ cell migration to CXCL12 was reduced (Fig 2A and Supplementary Fig 3H), suggesting a potential role for Abcc1 in GGG export. We then made Abcc1-deficient mice by using CRISPR/Cas9 to delete a segment of the gene previously shown to be essential for Abcc1 protein expression in mice (20) (Supplementary Fig 3C,D). These mice allowed us to assay production of GGG by Abcc1-deficient cells. GGG was detected at significantly reduced concentrations in the supernatants of stimulated Abcc1-deficient B cells compared to wildtype B cells (Fig 2B). These data strongly supported the conclusion that Abcc1 functions as a GGG transporter. Attempts to detect alterations in GGG abundance in

lymphoid tissues of Abcc1-deficient mice were confounded by the very low amounts present in these tissues in wild-type mice and by an inability to sample selectively the interstitial space. Analysis of bile collected from Abcc1-deficient mice showed a trend towards decreased GGG that did not reach significance (Supplementary Fig 3E), suggesting that additional transporters may contribute to GGG export in the liver.

To evaluate the role of Abcc1 in shaping the lymphoid tissue GGG gradient, P2RY8-expressing B cells were transferred into Abcc1-deficient mice and their littermate controls. P2RY8$^+$ B cells failed to localize to the GCs of pre-immunized Abcc1-deficient mouse spleens and LNs and instead were found throughout the IgD$^+$ region of the B cell follicle, a region P2RY8$^+$ cells are normally excluded from (Fig 3A, Supplementary Fig 3F,G). The distribution of P2RY8$^+$ cells in Abcc1-deficient mice mimicked the distribution of empty vector expressing control cells. These data indicated that Abcc1 has a non-redundant role in establishing the extracellular GGG distribution needed for P2RY8 function in B cell follicles.

B cells were an important source of GGG:

We took advantage of the critical role of Abcc1 in GGG export to determine the GGG-producing cell types necessary for follicle-center confinement of P2RY8-expressing cells. We generated chimeric mice in which Abcc1 sufficient or deficient BM was transferred into Abcc1 sufficient or deficient irradiated hosts. P2RY8$^+$ cells failed to cluster in the GCs of chimeric mice lacking Abcc1 in their hematopoietic compartment, but were able to localize in these regions in mice lacking Abcc1 only in their stromal compartment (Fig 3B, Supplementary Fig 4A,B), indicating hematopoietic Abcc1 is both necessary and sufficient for this GC localizing behavior. Interestingly, in mice lacking Abcc1 in the hematopoietic compartment, but with functional Abcc1 in the stromal compartment, P2RY8$^+$ cells failed to localize in the GC, but were not distributed evenly throughout the IgD$^+$ follicle like empty vector cells or P2RY8$^+$ cells transferred into completely Abcc1-deficient mice (Fig 3A,B). Instead, these P2RY8$^+$ cells were often found at the interface of the follicle and GC, ringing this region. This discrepancy between the P2RY8$^+$ cell localizing patterns in full Abcc1-deficient mice and mice with functional Abcc1 in their stromal compartment was especially clear when higher numbers of P2RY8$^+$ cells were transferred (Supplementary Fig 4A). This finding provided evidence that stromal cells are capable of exporting GGG and contributing to its overall distribution in tissue.

To determine if B cell expression of Abcc1 was necessary for GGG gradient generation, we made mixed chimeras using BM from μMT mice, which lack the ability to generate mature B cells. The μMT BM was mixed in a 3 to 1 ratio with Abcc1 sufficient or deficient BM to produce mice in which Abcc1 was completely absent from B cells, but present on other hematopoietic cell types and stromal cells. P2RY8$^+$ cells failed to cluster in the GC of these mice, instead ringing the GC region, as was seen in mice lacking Abcc1 in all but their stromal compartment (Fig 3C and Supplementary Fig 4C,D). These data indicated that B cells are the major hematopoietic source of GGG within lymphoid follicles.

P2RY8 expression in GC B cells leads to a suppressive effect on GC B cell growth, particularly in mouse PPs and mLNs (1). It is the loss of this growth repressive effect

that likely underlies the connection between P2RY8 mutations and development of BL and GCB-DLBCL in humans. Using chimeric mice generated with P2RY8-transduced BM, we found this effect to be dependent on Abcc1, with the loss of Abcc1 in the hematopoietic compartment being sufficient for abrogation of the GC B cell growth-repression phenotype in PPs (Fig 3D, Supplementary Fig 5C). We detected only a slight P2RY8-mediated suppressive effect on GC B cells in the spleen, but this also appeared Abcc1-dependent (Supplementary Fig 5B,C). The effect of P2RY8 on GC B cells in mLNs was more variable but again there was evidence of an Abcc1-dependent repressive effect (Supplementary Fig 5B,C). Interestingly, the PP and mLN data showed evidence of P2RY8 expression conferring a GC growth advantage when Abcc1 was selectively lacking in hematopoietic cells. Taking this finding together with the observation that P2RY8+ B cells tend to position at the perimeter of GCs in BM chimeras of this type (Fig 3B.C and Supplementary Fig 4C,D), we speculated that this location may be advantageous for GC cell growth. Overall, these data provided *in vivo* evidence that the growth regulatory actions of P2RY8, like the confinement actions, depend on engagement with GGG.

P2RY8 is located on a portion of the pseudoautosomal region of the X chromosome that has been lost in rodents[1]. With mice lacking a sequence orthologue of P2RY8, alterations of the GGG gradient may not be predicted to alter endogenous mouse B cell guidance or growth regulation. However, it remains possible that they respond to GGG through a distinct receptor. We therefore examined whether confinement of endogenous GC B cells was altered in Ggt5 or Abcc1 deficient mice. Previous work in mice lacking the GC confinement receptor S1pr2 or the downstream Gα13 protein has shown that one measure of reduced confinement is the increased presence of IgD^+ follicular B cells within the GC (1, 21). Staining of mLNs of Ggt5 and Abcc1 deficient mice showed that there was no increase in IgD^+ cells in the GC compared to wild-type controls (Supplementary Fig 6A). Sections from S1pr2 deficient control mice demonstrated the expected intermixing of follicular and GC B cells (Supplementary Fig 6A). Mice lacking Gα13 (but not S1pr2) suffer an extent of GC deconfinement that is sufficient to cause dissemination of GC B cells into the lymph[1]. Ggt5 and Abcc1 deficient mice, as well as Abcc1 chimeric mice, showed normal GC B cell frequencies upon sheep red blood cell (SRBC) immunization (Supplementary Fig 6B,C,D), and no dissemination of GC B cells into the lymph (Supplementary Fig 6E,F). We also tested the effect of combined loss of S1pr2 and disruption of the GGG gradient. Chimeric mice lacking S1pr2 in their hematopoietic compartment and Ggt5 in their radioresistant compartment showed no increased dissemination of GC B cells into the lymph compared to S1pr2-deficient control animals (Supplementary Fig 6E,F). These findings suggested that there is not a direct role for Ggt5 or Abcc1 in GC confinement of mouse B cells.

P2RY8 and GGG restrained lymphocyte homing to bone marrow:

In the course of evaluating the role of the GGG gradient in lymphoid organs via the transfer of P2RY8 expressing cells, we noted that activated $P2RY8^+$ polyclonal B cells were less represented in the BM after 24hrs compared to their initial cell representation upon transfer into the mouse (Fig 4A, Supplementary Fig 7A). This effect was not seen in the blood after 24hrs (Fig 4B), and when the representation of P2RY8 cells was compared between the blood and BM of individual animals, there was a clear defect in the homing of $P2RY8^+$

cells to the BM (Fig 4C). Polyclonal P2RY8$^+$ B cells were also less likely to be present in the spleen after 24hrs, though this difference was of a smaller magnitude than that seen in the BM (Supplementary Fig 7A,B). P2RY8$^+$ cell homing to inguinal or mLNs was comparable to the vector control cells (Supplementary Fig 7A,C,D). This notably decreased homing to the BM was not unique to B cells, as activated P2RY8-transduced polyclonal CD4$^+$ and CD8$^+$ T cells were also less likely to be found in the BM in comparison to control cells, at both 24hrs and 5 days following transfer (Fig 4A-C and Supplementary Fig 8A-D). While there was a decrease in P2RY8$^+$ CD8$^+$ T cell representation in the blood at 24hrs, this difference reversed after 5 days, and the representation of P2RY8$^+$ cells in the BM compared to the blood for CD8$^+$ T cells was consistent with the other lymphocytes examined. Furthermore, the inhibition of BM homing was dependent on the downstream effector of P2RY8, Gα13, as P2RY8-transduced B cells from mice deficient in this G protein demonstrated equal ability to home to the BM compared to empty vector control cells (Supplementary Fig 7E). The homing defect of P2RY8$^+$ cells was furthermore not unique to *in vitro* activated B or T cells, as in chimeric mice reconstituted with P2RY8 transduced BM, P2RY8$^+$ mature B cells, T cells, and NK cells were all less represented in the BM compared to the blood (Fig 4D, Supplementary Fig 9).

While fewer P2RY8$^+$ cells homed to the BM overall, the P2RY8$^+$ polyclonal B and T cells that did migrate to the BM were roughly two-fold more likely to be associated with the BM vasculature rather than in the BM parenchyma, based on their rapid *in vivo* staining with intravenously injected anti-CD45-PE (Fig. 4E, Supplementary Fig 10A-C. This quantification was also supported by two photon imaging of calvarial BM, where P2RY8+ cells were more abundant in locations overlapping with the vasculature (Supplementary Fig 11A,B). This finding suggested an inhibitory effect of P2RY8 as cells transit from the vasculature and make their way into the BM parenchyma. Mass spectrometry analysis of total mouse BM (cells and any interstitial fluid) established that GGG was detectable (Fig. 4F, Supplementary Fig 11D). An analysis of cell-free human BM aspirates drawn from three healthy donors established that GGG was also present in the interstitial space of human BM (Fig 4G and Supplementary Fig 11E). The difference in the amount of GGG detected in mouse and human BM most likely reflected the presence of considerable transudated plasma in the human aspirates. We were unable to detect GGG in human plasma by mass spectrometry. In accord with local production of GGG, many hematopoietic cells (as well as recirculating lymphocytes) in mouse BM (Immgen.org) and human BM (Human Cell Atlas scRNAseq (22)) express Abcc1 (Supplementary Fig 11C). Notably, P2RY8 was also expressed by many hematopoietic cells within human BM, while Ggt5 was strongly expressed by BM stromal cells.

To determine whether the decreased BM homing of P2RY8$^+$ cells was dependent on GGG, polyclonal B cells expressing P2RY8 or empty vector were transferred into mice deficient in Ggt5 or Abcc1. Interestingly, P2RY8$^+$ cells in mice deficient in Ggt5 showed a further reduced ability to home to the BM (Fig. 5A), perhaps reflecting stronger inhibition of P2RY8$^+$ cell entry due to elevated tissue concentrations of GGG. Importantly, deficiency in Abcc1 restored the BM homing ability of P2RY8$^+$ cells (Fig 5A). While loss of Ggt5 had an unclear effect on the intravascular partitioning of P2RY8$^+$ cells (Supplementary Fig 11F), Abcc1 deficiency notably abrogated the increased vascular presence of P2RY8$^+$ cells in the

BM (Fig 5B). Abcc1 deficiency also abrogated the smaller intravascular bias of P2RY8$^+$ cells seen in the spleen (Supplementary Fig 12A,B).

Given the loss of hematopoietic Abcc1 was sufficient to disrupt the P2RY8$^+$ cell localizing behavior in the GC, we aimed to determine if the same was true for the GGG-mediated restriction of cell access to the BM. Thus, we transferred P2RY8$^+$ cells into chimeras reconstituted with the series of combinations of Abcc1 sufficient and deficient BM. The results showed that Abcc1 was required only on hematopoietic cells for the inhibition of P2RY8$^+$ cell migration to the BM (Fig 5C). Notably, mice lacking Abcc1 in their stromal compartment but retaining Abcc1 in their hematopoietic compartment exhibited an even stronger block in the BM homing of P2RY8$^+$ cells compared to control mice. Moreover, while the intravascular bias of P2RY8$^+$ cells in the BM of these chimeric mice (Fig 5D) mirrored the phenotype seen at the whole tissue level, the vascular bias seen in mice lacking Abcc1 in just their stromal compartment was on average 15-fold higher, vs the approximately two-fold increase seen in non-chimeric mice. These data suggest a complexity in the shape of the BM GGG gradient and the cell types contributing to its organization. Abcc1-dependent reduced homing to the BM was not unique to *in vitro* activated B cells, as mature B cells, CD4$^+$ T cells, CD8$^+$ T cells, and NK cells in mice reconstituted with P2RY8-transduced BM also showed a reduced presence in the BM, which was dependent on Abcc1 (Fig 5E, Supplementary Fig 9). Notably, for B cells and CD4$^+$ T cells in this system, there was an increased presence of P2RY8$^+$ cells in the BM of mice lacking Abcc1 in their hematopoietic system. These data suggested that when stromal cells are the only source of extracellular GGG, P2RY8$^+$ cells show enhanced entry into, or reduced exit from, the BM.

Human T cell homing to bone marrow was restricted by P2RY8:

Finally, we sought to test the function of endogenous P2RY8 in human cells *in vivo* using the NOD-scid-gamma (NSG) mouse model (23). Currently there are no well-established protocols for studying human GC formation in humanized mice (24). However, our finding that P2RY8 expression on mouse lymphocytes led to decreased homing to the BM gave us the opportunity to test whether endogenous P2RY8 on human cells regulated BM homing in NSG mice. Using CRISPR/Cas9, we ablated P2RY8 in stimulated human CD4 and CD8 T cells isolated from four blood donors. Three days following CRISPR editing, these cells had a confirmed editing efficiency of above 95% by TIDE analysis in three out of four donors (Fig. 6A and Supplementary Fig 13A,B), and protein staining of cellular P2RY8 levels via flow cytometry showed decreased staining in both CD4$^+$ and CD8$^+$ edited T cells compared to control cells (Fig 6B). The edited T cell cultures were tested for their ability to sense GGG during migration to CXCL12, and while control T cells showed partial inhibition in their migration to CXCL12 upon addition of 100 or 1000 nM GGG, P2RY8 KO T cells were not inhibited in their migration (Fig 6C,D and Supplementary Fig 13C,D). This finding is notable, as it extends the sites where there is evidence for P2RY8-GGG action in human T cells beyond Tfh cells (7), to T cells that have been activated under non-polarizing conditions. Although the degree of migration inhibition is smaller than observed in previous studies for GC B and Tfh cells, it should be noted that *in vitro* migration assays can be influenced by many parameters (such as cell activation status) and their magnitude often

does not equate to the magnitude of the *in vivo* response. CFSE or CTV labeled P2RY8 KO and control cells were then transferred intravenously to NSG mice. A time point of 48hrs was chosen to examine T cell homing to the BM in NSG mice as an initial time course experiment showed that human T cells had already significantly accumulated in the BM by this time (Supplementary Fig 13G). At 48hrs following transfer, P2RY8 KO T cells were more likely to be found in the BM than controls cells, while this representation bias was not seen for cells in the blood (Fig 6E, Supplementary Fig 13E,F). This effect was independent of CTV or CFSE labeling (Supplementary Fig 13H) and correlated with the editing efficiency of each T cell donor culture via TIDE analysis (Fig 6F). These results indicated that loss of endogenous levels of P2RY8 on human T cells is sufficient to increase homing of these cells to the BM.

Discussion

In this study we defined key requirements for the establishment of extracellular GGG distribution in lymphoid tissues. We showed that GGG was an endogenous substrate for cell membrane transporter Abcc1 and that Abcc1 was used by both hematopoietic and non-hematopoietic cells to export GGG. Additionally, we showed that Ggt5 was necessary for extracellular GGG catabolism in lymphoid tissues. Our data indicated that Abcc1 and Ggt5 acted in concert to support P2RY8-mediated confinement of cells to the GC, and Abcc1 was also needed for growth regulation of P2RY8^{+} GC B cells, most notably in PPs. Furthermore, we showed that extracellular GGG was generated in an Abcc1-dependent manner in the BM, and that P2RY8 could restrict lymphocyte accumulation in the BM parenchyma (Fig 7).

Our earlier work (1) establishes that although rodents lack P2RY8, they produce the P2RY8 ligand GGG, a finding that we build on here. We make the inference that the GGG-P2RY8 pathway functions in humans in a manner that is closely modeled by our mouse studies for the following reasons. First, P2RY8 loss-of-function mutations in lymphoma patients are associated with GC B cell over-growth and dissemination (1), leading to the prediction that P2RY8 promoted GC B cell growth restraint and confinement; we observed that P2RY8 was sufficient to have these effects in the mouse. Second, Ggt5 expression by FDCs is conserved between humans and mice (7). Third, Abcc1 is widely expressed by human immune cells, similar to its expression in the mouse (this study and Immgen.org). Finally, our mass spectrometry measurements show comparable GGG abundance in mouse lymph nodes and human tonsil (7) and that GGG is present in mouse and human BM. Taken together, these observations suggest efforts to decipher the biology of this ligand-receptor system using mouse models will help illuminate the role of P2RY8 in human physiology and disease.

ABCC1 is intensely studied for its ability to transport a diversity of drugs and xenobiotics, often as glutathione conjugates, though it has only one well-defined endogenous substrate *in vivo*, LTC4 (12). We now add GGG as another endogenous substrate of ABCC1. ABCC1 transporter activity is not known to be regulated or gated beyond its ATP requirement (12, 25). Instead, the expression pattern of the transporter is likely to be a key determinant of where GGG export occurs. The widespread expression of ABCC1 suggests that most cell types within lymphoid tissues have the capacity to export GGG. The key factors determining GGG distribution may then be the enzymes involved in GGG synthesis and degradation.

While our gene knockout data showed a critical role for Abcc1 in generating extracellular GGG in lymphoid tissues that can act on P2RY8, we continued to observe significant amounts of GGG in the bile of Abcc1-deficient mice, likely indicating that at least one additional Abcc transporter is active in GGG export. In this regard, it is notable that Abcc2 and Abcc3, close homologs of Abcc1, are particularly abundant in the liver (BioGPS.org).

We show that follicular B cells were a necessary source of GGG to mediate the GC confinement of P2RY8$^+$ B cells, identifying a form of crosstalk between different B cell subsets in lymphoid tissues. In mice lacking Abcc1 only in hematopoietic cells or fully deficient in B cells, P2RY8$^+$ B cells were not confined to GCs but they were also not uniformly distributed in follicles; rather they had a propensity to distribute at the follicle-GC boundary. We speculate that under normal conditions, follicular GGG is produced by B cells and stromal cells, and this achieves a high concentration that penetrates some distance into the Ggt5$^+$ FDC network that occupies the GC. This ‘gradient’ helps promote confinement of P2RY8$^+$ cells within the GC. When stromal cells are the only source of GGG, the lower amounts of GGG may be more readily degraded by the Ggt5$^+$ FDCs with little penetration into the GC. Under these conditions P2RY8 is only sufficient to position activated B cells at the follicle-GC interface.

Within lymphoid follicles, Ggt5 was most highly expressed by FDCs. The previous finding that FDCs are required for P2RY8-mediated confinement of cells to the follicle center and to GCs (8) is consistent with them having a critical role in GGG catabolism. Ggt5 is also detectable on stromal cells in the T zone of LNs and human tonsil (7), and the transcript is present in naïve T cells and dendritic cells (Immgen.org). Whether GGG-P2RY8 signaling has a role in regions of secondary lymphoid tissue outside the follicle has not yet been determined. We speculate that GGG distribution may also be tightly regulated in the T zone, allowing GGG to influence cell compartmentalization within this zone. Moreover, while we established that Ggt5 has a non-redundant role in catabolism of GGG in lymphoid tissues, our findings do not exclude possible contributions by other Ggt family members in GGG catabolism.

Abcc1 and Ggt5 regulation of cell trafficking to the BM identified a role for P2RY8 outside the GC. The BM is a significant site of lymphocyte and plasma cell homing. Multiple studies have characterized the presence of memory T cells in mouse and human BM, and it has been suggested that they are an important memory reservoir in both protective and autoimmune contexts (26)·(27)·(28). The intravascular labeling experiments presented here indicated that P2RY8-expressing cells were ultimately impeded in their movement from blood vessels into the BM parenchyma, failing to accumulate in the parenchyma after 24hrs. VCAM1 is required for homing of circulating B and T cells into the BM, facilitating the adherence of lymphocytes to the vessel wall (29)·(28). The requirements for lymphocyte transendothelial migration into the BM after sticking are not fully characterized, but CXCR4 and CXCL12 play a role in this process(28). In accordance with P2RY8’s established role in inhibiting migration towards chemoattractants, we speculate that P2RY8 may act to antagonize the transmigration step, counteracting the influence of chemoattractants and thereby gating lymphocyte access to the BM. It may also be the case that P2RY8-expressing cells encounter GGG after they have migrated through the endothelium, leading them to

reverse transmigrate back into the vasculature. In addition to their role in lymphocyte transmigration, CXCR4 and CXCL12 are also important in homing of plasma cells to the BM (30). It will be important in future work to determine if newly generated human plasmablasts express sufficient amounts of P2RY8 to potentially restrict their accumulation in the BM and to understand what factors alter P2RY8 expression in BM tropic cells. Given the widespread expression of P2RY8 and ABCC1 in human BM cells detected by scRNAseq analysis, and the expression of GGT5 by subsets of BM stromal cells (31), we speculate that the receptor may also have influences on cell distribution in the BM parenchyma and thus on hematopoiesis. Future studies will be needed to address this topic. Additionally, while we focused our homing studies on the BM, our finding that P2RY8 expression reduced homing to the spleen suggests the receptor may restrain P2RY8+ cell accumulation in other tissues.

P2RY8 and GNA13 are frequently mutated in GC-derived lymphomas (1–6). The Abcc1 dependence of the growth repressive influence of P2RY8 on GC B cell responses is consistent with GGG acting *in vivo* on GC B cells to repress Akt (and possibly other pro-growth signaling pathways). It is notable that GC-derived lymphomas retain an extensive FDC network at least through the early stages of disease (32). A large FDC network would be expected to maintain low GGG levels, acting as an alternative mechanism to P2RY8 or GNA13 mutation to limit P2RY8-mediated repression of growth-promoting pathways. BM involvement presents in a portion of GCB-DLBCL patients and is a predictor of poor clinical outcome (33). Mutations in P2RY8 and GNA13 may not only lead to loss of GC confinement and GC B cell growth regulation, but also favor the recruitment of malignant cells to the BM. In another cancer context, efforts are being pursued to antagonize the multidrug transporter activity of ABCC1 in an attempt to improve the success of chemotherapies (12, 34). The role of ABCC1 in transporting GGG will be important to consider in the context of these efforts. It will also be of interest to determine whether the polymorphisms that have been described in ABCC1 (34, 35) lead to alterations in GGG export. The basis for the stronger effect of P2RY8 in restraining GC B cell growth in PPs than in spleen and mLNs is not yet known but is in accord with earlier findings (1). We speculate that different combinations of factors may contribute to GC growth control in different lymphoid organs, and P2RY8 may play a particularly prominent role in the regulation of GC growth in chronically inflamed mucosal tissues, such as PPs, tonsils and adenoids. Moreover, it should be kept in mind that the mouse model may only be effective in revealing a fraction of P2RY8's endogenous functions in humans. For example, the importance of P2RY8 in human LNs is strongly suggested by the evidence that GCB-DLBCL and BL frequently emerge in these tissues(36).

Finally, while we highlighted influences of the P2RY8-GGG axis on lymphocyte organization in secondary lymphoid organs and trafficking to the BM, we note that ABCC1 is widely expressed in tissues and GGG can be made by many cell and tissue types (7). Therefore, the findings described here are anticipated to provide a foundation for understanding the broader influences of GGG and P2RY8 in the human immune system.

Materials and Methods

Study Design

The aim of this study was to characterize the enzymatic and transporter requirements for P2RY8-dependent positioning of B cells in GCs. In the course of our studies, we discovered a function for P2RY8 in restraining lymphocyte homing to the BM. Most of the experiments consisted of enumeration of population frequencies by flow cytometry, assessment of cell distribution using immunofluorescence, and quantitation of GGG abundance using a cell migration-based bioassays or LC-MS/MS. Littermate comparisons were used for all mouse studies unless otherwise indicated. Control and experimental treatments were administered to age- and sex-matched mice that had been allocated to groups randomly, with sample sizes chosen based on previous experience and available co-caged littermates to obtain reproducible results. The investigators were not blinded, with the exception of certain two photon imaging analysis. Experimental replication is indicated in the figure legends. No data was excluded from analysis with one exception: a single mouse failed to reconstitute with transduced BM following irradiation and was thus excluded from the analysis depicted in Figure 3D and 5E.

Mice

Mice were bred in an internal colony and 6–12-week-old mice of both sexes were used. Ggt5 and Abcc1 lines were internally generated and bred. μMT mice (B6.129S2-*Ighm*^{tm1Cgn}/J) were obtained from C. Allen at UCSF, and Nod *scid* gamma (NSG) mice (NOD.Cg-*Prkdc*^{scid} *Il2rg*^{tm1Wjl}/SzJ) were obtained from A. Marson and Q. Tang at UCSF. CD45.1 B6 mice (B6.SJL-*Ptprc*a*Pepc*b/BoyCrCrl) were bred internally from founders ordered from JAX, or were purchased from National Cancer Institute at Charles River at age 6–8 wks. Littermate controls were used for experiments, mice were allocated to control and experimental groups randomly, and sample sizes were chosen based on previous experience and available co-caged littermates to obtain reproducible results. Animals were housed in a pathogen-free environment in the Laboratory Animal Resource Center at UCSF, and all experiments conformed to ethical principles and guidelines that were approved by the Institutional Animal Care and Use Committee.

Generation of Ggt5−/− and Abcc1−/− mice

In brief, Ggt5−/− and Abcc1−/− mice were generated using CRISPR-EZ (37). The targeted region for each knockout line was selected to replicate previously reported mouse lines. These lines were shown to lack functional Ggt5 and Abcc1 (14, 20). More detailed methodology can be found in the supplemental material.

Bone marrow chimeras

In brief, freshly harvested BM, or BM transduced with MSCV-P2RY8-GFP or MSCV-EV-GFP, was transferred into irradiated mice. More detailed methodology can be found in the supplemental material.

Retroviral transduction and activation of lymphocytes

In brief, freshly isolated mouse B or T cells were activated and transduced with MSCV-P2RY8-GFP or MSCV-EV-GFP. More detailed methodology can be found in the supplemental material.

Immunofluorescence

Spleens were fixed in 4% PFA for 2 hr at 4 °C, washed with PBS, submerged in 30% sucrose overnight and embedded in OCT. Cryosections of 7 μm were dried for 1 hr at room temperature and rehydrated in PBS containing 0.1% fatty acid-free BSA for 10 min. To track the position of GFP-transduced B cells, a solution consisting of 1% NMS and 1:100 AF488-conjugated rabbit anti-GFP (Invitrogen, Cat#A21311), 1:100 biotin-conjugated anti-mouse CD35/CR1 (BD Bioscience, Cat # 553816), and 1:100 AF647-conjugated anti-mouse IgD (Biolegend, Cat#405708) was used to label transduced B cells, FDCs, and endogenous naive B cells, respectively. To examine the GC confinement of endogenous mouse B cells, a solution consisting of 1% NMS and 1:100 biotin-conjugated GL7 (Thermofisher, Cat#13–5902-81) and 1:100 AF647-conjugated anti-mouse IgD (Biolegend, Cat#405708) was used to label GC B cells and naïve B cells, respectively. These solutions were incubated with the slides overnight at 4°C. The slides were then washed in PBS and stained with AF555-conjugated streptavidin (Life Technologies, Cat#S-21381) for 1 hr at room temperature, and images were captured with a Zeiss AxioObserver Z1 inverted microscope. For the assessment of P2RY8 effects on cell distribution within spleen and LNs, we compared sections that contained similar frequencies of transferred empty vector or P2RY8 transduced cells.

Two photon microscopy

In brief, activated B cells transduced with EV-GFP or P2RY8-GFP were transferred iv into mice, and 24 hrs later the BM of the calvaria was imaged. Mice were injected with tetramethylrhodamine conjugated dextran to delineate the vasculature. Acquired images were analyzed with Imaris software (v.9.6). More detailed methodology can be found in the supplemental material.

Cell lines and treatments

In brief, HEK293T and WEHI-231 were grown in standard culture media. HEK293T cells were treated with MK571 (Caymen Chemical, Cat #70720) for 16 hr and then the media was collected for use in the P2RY8+ WEHI-231 bioassay. More detailed methodology can be found in the supplemental material.

Migration inhibition transwell bioassay

In brief, a transwell migration assay was performed as previously described with WEHI-231 cells (7). The cells were allowed to migrate for 3 hrs, after which the cells in the bottom well were counted by flow cytometry. More detailed methodology can be found in the supplemental material.

Migration assay of human T Cells

CRISPR edited human T cells were collected 3 days after editing. P2RY8 KO cells were labele with 1:2000 CFSE (Invitrogen) and AAVS KO control cells were labeled with 1:2000 CTV (Fisher) and then mixed at a 1:1 ratio. In some experiments this labeling was reversed. The cells were resuspended in migration medium at approximately 2×10^6 cells/ml and resensitized for 10 min in a 37°C water bath. Recombinant human CXCL12 (Peprotech) was diluted to 100 ng/ml in migration medium and synthetic GGG was added to aliquots via serial dilution from 1μM down to 10nM GGG. Transwell assays were performed as described in Supplementary Methods. To assess migration inhibition, the number of P2RY8 KO and AAVS KO cells that migrated to the bottom of each well was compared to the number of P2RY8 KO and AAVS KO cells that migrated to CXCL12 alone. The number of P2RY8 KO cells was also directly compared in a ratio to the number of AAVS KO cells that migrated in each well, a value that was normalized to the ratio in the wells receiving CXCL12 alone. The calculations as performed on the raw data can be viewed in Supplementary Table 3: Raw Data.

Immunizations, intravascular labeling and tissue collection

All immunizations were performed with intraperitoneal injection of 2×10^8 SRBC (Colorado Serum Company) in a volume of 400 μL. For studies of polyclonal P2RY8+ cell localization in the spleen or homing to the BM, mice were immunized on Day 0, cells were transferred in on Day 5, and tissues were harvested on Day 6 (or Day 11 for the analysis of T cells 5 days after transfer). For studies with chimeric mice in which Abcc1+/+ or −/− BM had been transduced with EV-GFP or P2RY8-GFP and used to reconstitute congenically marked recipients, mice were immunized with SRBC on Day 0 and Day 7, and then tissues were harvested on Day 10. *In vivo* pulse labeling was with 1 μg of PE-conjugated anti-CD45.2 injected i.v., and mice were analyzed after 3 min (38, 39). Immune cells from spleen, mLNs, BM, PPs and blood were isolated as previously described (21). Lymph was collected from the cysterna chyli via fine glass micropipette as previously described (40).

CRISPR T Cell knockdown and adoptive transfer

In brief, primary human $CD3^+$ T cells were isolated by negative selection, activated, and cultured for 2 days. Cells were then edited with guides targeted against P2RY8 and AAVS (as a control), followed by culture for another 4 days. Aliquots of cells were then set aside for genomic DNA extraction, PCR, and Sanger sequencing to determine editing efficiency quantified by TIDE analysis (tide.nki.nl) as previously described (41). CRISPR edited P2RY8 KO and AAVS KO control human T cells were labeled with CFSE and CTV, mixed at a 1:1 ratio, and injected iv into NSG mice. More detailed methodology can be found in the supplemental material.

Cell surface flow cytometry staining

In brief, cells were prepared for flow cytometry as previously described (7). See Supplementary Table 2 for antibodies used. Flow cytometry data were analyzed using Flowjo (v.10.7.1). More detailed methodology can be found in the supplemental material.

P2RY8 protein flow cytometry staining

In brief, cells were fixed in 1.6% PFA and stained with an anti-human-P2RY8 antibody (Sigma, HPA003631). More detailed methodology can be found in the supplemental material.

GGG extraction and mass spectrometry

In brief, GGG was measured in the supernatant of cell cultures and tissue using the previously described LC-MS/MS protocol (7). More detailed methodology can be found in the supplemental material.

Statistics

Prism software (GraphPad v.8.4.2) was used for all statistical analyses. The statistical tests used are specified in the figure legends. Two-tailed unpaired t-tests were performed when comparing only two groups, and ordinary one-way ANOVA using Tukey's multiple comparisons test was performed when comparing one variable across multiple groups. A two-tailed paired t-test was performed when comparing paired BM and blood samples from NSG mice that received CRISPR-edited human T cells. In summary graphs, points indicate individual samples and horizontal lines are means. Levels of significance were defined as *P < 0.05, **P < 0.01, ***P < 0.001, ****P < 0.0001.

Supplementary Material

Refer to Web version on PubMed Central for supplementary material.

Acknowledgments:

For access to μMT mice and Nod *scid* gamma mice we thank C. Allen and Q. Tang at UCSF, respectively. For advice regarding calvaria imaging, we thank Joao Pereira.

Funding:

This work was funded by National Institute of Allergy and Infectious Disease grant to A.E.G. (F30AI150061). F.D.W. is supported by a CRI Irvington postdoctoral fellowship. D.N.N. is supported by NIH grants L40AI140341 and K08AI153767 and the CIRM Alpha Stem Cell Clinic Fellowship. A.M. holds a Career Award for Medical Scientists from the Burroughs Wellcome Fund, is an investigator at the Chan-Zuckerberg Biohub and is a recipient of The Cancer Research Institute (CRI) Lloyd J. Old STAR grant. The Marson lab has received funds from the Innovative Genomics Institute (IGI) and the Parker Institute for Cancer Immunotherapy (PICI). J.G.C. is an HHMI investigator, recipient of a UCSF PBBR Award, and is also supported by a National Institutes of Health USA Grant (R01 AI045073).

Data and materials availability:

All data needed to evaluate the conclusions in the paper are present in the paper or the Supplementary Materials.

References and Notes:

1. Muppidi JR, Schmitz R, Green JA, Xiao W, Larsen AB, Braun SE, An J, Xu Y, Rosenwald A, Ott G, Gascoyne RD, Rimsza LM, Campo E, Jaffe ES, Delabie J, Smeland EB, Braziel RM, Tubbs RR, Cook JR, Weisenburger DD, Chan WC, Vaidehi N, Staudt LM, Cyster JG, Loss of signalling

via Galpha13 in germinal centre B-cell-derived lymphoma. Nature516, 254–258 (2014). [PubMed: 25274307]

2. Lohr JG, Stojanov P, Lawrence MS, Auclair D, Chapuy B, Sougnez C, Cruz-Gordillo P, Knoechel B, Asmann YW, Slager SL, Novak AJ, Dogan A, Ansell SM, Link BK, Zou L, Gould J, Saksena G, Stransky N, Rangel-Escareno C, Fernandez-Lopez JC, Hidalgo-Miranda A, Melendez-Zajgla J, Hernandez-Lemus E, Schwarz-Cruz y Celis A, Imaz-Rosshandler I, Ojesina AI, Jung J, Pedamallu CS, Lander ES, Habermann TM, Cerhan JR, Shipp MA, Getz G, Golub TR, Discovery and prioritization of somatic mutations in diffuse large B-cell lymphoma (DLBCL) by whole-exome sequencing. Proc. Natl. Acad. Sci. U. S. A. 109, 3879–3884 (2012). [PubMed: 22343534]
3. Morin RD, Mungall K, Pleasance E, Mungall AJ, Goya R, Huff RD, Scott DW, Ding J, Roth A, Chiu R, Corbett RD, Chan FC, Mendez-Lago M, Trinh DL, Bolger-Munro M, Taylor G, Hadj Khodabakhshi A, Ben-Neriah S, Pon J, Meissner B, Woolcock B, Farnoud N, Rogic S, Lim EL, Johnson NA, Shah S, Jones S, Steidl C, Holt R, Birol I, Moore R, Connors JM, Gascoyne RD, Marra MA, Mutational and structural analysis of diffuse large B-cell lymphoma using whole-genome sequencing. Blood122, 1256–1265 (2013). [PubMed: 23699601]
4. Forbes SA, Bindal N, Bamford S, Cole C, Kok CY, Beare D, Jia M, Shepherd R, Leung K, Menzies A, Teague JW, Campbell PJ, Stratton MR, Futreal PA, COSMIC: mining complete cancer genomes in the Catalogue of Somatic Mutations in Cancer. Nucleic Acids Res. 39, D945–950 (2011). [PubMed: 20952405]
5. Schmitz R, Wright GW, Huang DW, Johnson CA, Phelan JD, Wang JQ, Roulland S, Kasbekar M, Young RM, Shaffer AL, Hodson DJ, Xiao W, Yu X, Yang Y, Zhao H, Xu W, Liu X, Zhou B, Du W, Chan WC, Jaffe ES, Gascoyne RD, Connors JM, Campo E, Lopez-Guillermo A, Rosenwald A, Ott G, Delabie J, Rimsza LM, Tay Kuang Wei K, Zelenetz AD, Leonard JP, Bartlett NL, Tran B, Shetty J, Zhao Y, Soppet DR, Pittaluga S, Wilson WH, Staudt LM, Genetics and Pathogenesis of Diffuse Large B-Cell Lymphoma. N. Engl. J. Med. 378, 1396–1407 (2018). [PubMed: 29641966]
6. Kridel R, Chan FC, Mottok A, Boyle M, Farinha P, Tan K, Meissner B, Bashashati A, McPherson A, Roth A, Shumansky K, Yap D, Ben-Neriah S, Rosner J, Smith MA, Nielsen C, Gine E, Telenius A, Ennishi D, Mungall A, Moore R, Morin RD, Johnson NA, Sehn LH, Tousseyn T, Dogan A, Connors JM, Scott DW, Steidl C, Marra MA, Gascoyne RD, Shah SP, Histological Transformation and Progression in Follicular Lymphoma: A Clonal Evolution Study. PLoS Med. 13, e1002197 (2016). [PubMed: 27959929]
7. Lu E, Wolfreys FD, Muppidi JR, Xu Y, Cyster JG, S-Geranylgeranyl-L-glutathione is a ligand for human B cell-confinement receptor P2RY8. Nature567, 244–248 (2019). [PubMed: 30842656]
8. Muppidi JR, Lu E, Cyster JG, The G protein-coupled receptor P2RY8 and follicular dendritic cells promote germinal center confinement of B cells, whereas S1PR3 can contribute to their dissemination. J. Exp. Med. 212, 2213–2222 (2015). [PubMed: 26573295]
9. Cyster JG, Allen CDC, B Cell Responses: Cell Interaction Dynamics and Decisions. Cell177, 524–540 (2019). [PubMed: 31002794]
10. Lu E, Cyster JG, G-protein coupled receptors and ligands that organize humoral immune responses. Immunol. Rev. 289, 158–172 (2019). [PubMed: 30977196]
11. Heisterkamp N, Groffen J, Warburton D, Sneddon TP, The human gamma-glutamyltransferase gene family. Hum. Genet. 123, 321–332 (2008). [PubMed: 18357469]
12. Cole SP, Targeting multidrug resistance protein 1 (MRP1, ABCC1): past, present, and future. Annu. Rev. Pharmacol. Toxicol. 54, 95–117 (2014). [PubMed: 24050699]
13. Slot AJ, Molinski SV, Cole SP, Mammalian multidrug-resistance proteins (MRPs). Essays Biochem. 50, 179–207 (2011). [PubMed: 21967058]
14. Shi ZZ, Han B, Habib GM, Matzuk MM, Lieberman MW, Disruption of gamma-glutamyl leukotrienase results in disruption of leukotriene D(4) synthesis in vivo and attenuation of the acute inflammatory response. Mol. Cell. Biol. 21, 5389–5395 (2001). [PubMed: 11463821]
15. Carter BZ, Wiseman AL, Orkiszewski R, Ballard KD, Ou CN, Lieberman MW, Metabolism of leukotriene C4 in gamma-glutamyl transpeptidase-deficient mice. J. Biol. Chem. 272, 12305–12310 (1997). [PubMed: 9139674]
16. Hayes JD, Flanagan JU, Jowsey IR, Glutathione transferases. Annu. Rev. Pharmacol. Toxicol. 45, 51–88 (2005). [PubMed: 15822171]

17. Shimizu T, Lipid mediators in health and disease: enzymes and receptors as therapeutic targets for the regulation of immunity and inflammation. Annu. Rev. Pharmacol. Toxicol. 49, 123–150 (2009). [PubMed: 18834304]

18. Chen XS, Sheller JR, Johnson EN, Funk CD, Role of leukotrienes revealed by targeted disruption of the 5-lipoxygenase gene. Nature372, 179–182 (1994). [PubMed: 7969451]

19. Koley D, Bard AJ, Inhibition of the MRP1-mediated transport of the menadione-glutathione conjugate (thiodione) in HeLa cells as studied by SECM. Proc. Natl. Acad. Sci. U. S. A. 109, 11522–11527 (2012). [PubMed: 22679290]

20. Lorico A, Rappa G, Finch RA, Yang D, Flavell RA, Sartorelli AC, Disruption of the murine MRP (multidrug resistance protein) gene leads to increased sensitivity to etoposide (VP-16) and increased levels of glutathione. Cancer Res. 57, 5238–5242 (1997). [PubMed: 9393741]

21. Green JA, Suzuki K, Cho B, Willison LD, Palmer D, Allen CD, Schmidt TH, Xu Y, Proia RL, Coughlin SR, Cyster JG, The sphingosine 1-phosphate receptor S1P(2) maintains the homeostasis of germinal center B cells and promotes niche confinement. Nat. Immunol. 12, 672–680 (2011). [PubMed: 21642988]

22. Hay SB, Ferchen K, Chetal K, Grimes HL, Salomonis N, The Human Cell Atlas bone marrow single-cell interactive web portal. Exp. Hematol. 68, 51–61 (2018). [PubMed: 30243574]

23. Lee J, Brehm MA, Greiner D, Shultz LD, Kornfeld H, Engrafted human cells generate adaptive immune responses to Mycobacterium bovis BCG infection in humanized mice. BMC immunology14, 53 (2013). [PubMed: 24313934]

24. Li Y, Masse-Ranson G, Garcia Z, Bruel T, Kok A, Strick-Marchand H, Jouvion G, Serafini N, Lim AI, Dusseaux M, Hieu T, Bourgade F, Toubert A, Finke D, Schwartz O, Bousso P, Mouquet H, Di Santo JP, A human immune system mouse model with robust lymph node development. Nat. Methods15, 623–630 (2018). [PubMed: 30065364]

25. Wiese M, Stefan SM, The A-B-C of small-molecule ABC transport protein modulators: From inhibition to activation-a case study of multidrug resistance-associated protein 1 (ABCC1). Med. Res. Rev39, 2031–2081 (2019). [PubMed: 30941807]

26. Di Rosa F, Gebhardt T, Bone Marrow T Cells and the Integrated Functions of Recirculating and Tissue-Resident Memory T Cells. Front Immunol7, 51 (2016). [PubMed: 26909081]

27. Collins N, Han SJ, Enamorado M, Link VM, Huang B, Moseman EA, Kishton RJ, Shannon JP, Dixit D, Schwab SR, Hickman HD, Restifo NP, McGavern DB, Schwartzberg PL, Belkaid Y, The Bone Marrow Protects and Optimizes Immunological Memory during Dietary Restriction. Cell178, 1088–1101 e1015 (2019). [PubMed: 31442402]

28. Mazo IB, Honczarenko M, Leung H, Cavanagh LL, Bonasio R, Weninger W, Engelke K, Xia L, McEver RP, Koni PA, Silberstein LE, von Andrian UH, Bone marrow is a major reservoir and site of recruitment for central memory CD8+ T cells. Immunity22, 259–270 (2005). [PubMed: 15723813]

29. Koni PA, Joshi SK, Temann UA, Olson D, Burkly L, Flavell RA, Conditional Vascular Cell Adhesion Molecule 1 Deletion in Mice. Impaired lymphocyte migration to bone marrow. J. Exp. Med. 193, 741–754. (2001). [PubMed: 11257140]

30. Cyster JG, Homing of antibody secreting cells. Immunol. Rev. 194, 48–60 (2003). [PubMed: 12846807]

31. Baryawno N, Przybylski D, Kowalczyk MS, Kfoury Y, Severe N, Gustafsson K, Kokkaliaris KD, Mercier F, Tabaka M, Hofree M, Dionne D, Papazian A, Lee D, Ashenberg O, Subramanian A, Vaishnav ED, Rozenblatt-Rosen O, Regev A, Scadden DT, A Cellular Taxonomy of the Bone Marrow Stroma in Homeostasis and Leukemia. Cell177, 1915–1932 e1916 (2019). [PubMed: 31130381]

32. Carbone A, Gloghini A, Follicular dendritic cell pattern in early lymphomas involving follicles. Adv. Anat. Pathol. 21, 260–269 (2014). [PubMed: 24911251]

33. Sehn LH, Scott DW, Chhanabhai M, Berry B, Ruskova A, Berkahn L, Connors JM, Gascoyne RD, Impact of concordant and discordant bone marrow involvement on outcome in diffuse large B-cell lymphoma treated with R-CHOP. J. Clin. Oncol. 29, 1452–1457 (2011). [PubMed: 21383296]

34. Kunicka T, Soucek P, Importance of ABCC1 for cancer therapy and prognosis. Drug Metab. Rev. 46, 325–342 (2014). [PubMed: 24670052]

35. Yin J, Zhang J, Multidrug resistance-associated protein 1 (MRP1/ABCC1) polymorphism: from discovery to clinical application. Zhong Nan Da Xue Xue Bao Yi Xue Ban36, 927–938 (2011). [PubMed: 22086004]

36. Carbone A, Gloghini A, Cabras A, Elia G, The Germinal centre-derived lymphomas seen through their cellular microenvironment. Br. J. Haematol. 145, 468–480 (2009). [PubMed: 19344401]

37. Chen S, Lee B, Lee AY, Modzelewski AJ, He L, Highly Efficient Mouse Genome Editing by CRISPR Ribonucleoprotein Electroporation of Zygotes. J. Biol. Chem. 291, 14457–14467 (2016). [PubMed: 27151215]

38. Pereira JP, An J, Xu Y, Huang Y, Cyster JG, Cannabinoid receptor 2 mediates the retention of immature B cells in bone marrow sinusoids. Nat. Immunol. 10, 403–411 (2009). [PubMed: 19252491]

39. Beck TC, Gomes AC, Cyster JG, Pereira JP, CXCR4 and a cell-extrinsic mechanism control immature B lymphocyte egress from bone marrow. J. Exp. Med. 211, 2567–2581 (2014). [PubMed: 25403444]

40. Matloubian M, Lo CG, Cinamon G, Lesneski MJ, Xu Y, Brinkmann V, Allende ML, Proia RL, Cyster JG, Lymphocyte egress from thymus and peripheral lymphoid organs is dependent on S1P receptor 1. Nature427, 355–360 (2004). [PubMed: 14737169]

41. Brinkman EK, Chen T, Amendola M, van Steensel B, Easy quantitative assessment of genome editing by sequence trace decomposition. Nucleic Acids Res. 42, e168 (2014). [PubMed: 25300484]

42. Nguyen DN, Roth TL, Li PJ, Chen PA, Apathy R, Mamedov MR, Vo LT, Tobin VR, Goodman D, Shifrut E, Bluestone JA, Puck JM, Szoka FC, Marson A, Polymer-stabilized Cas9 nanoparticles and modified repair templates increase genome editing efficiency. Nat. Biotechnol. 38, 44–49 (2020). [PubMed: 31819258]

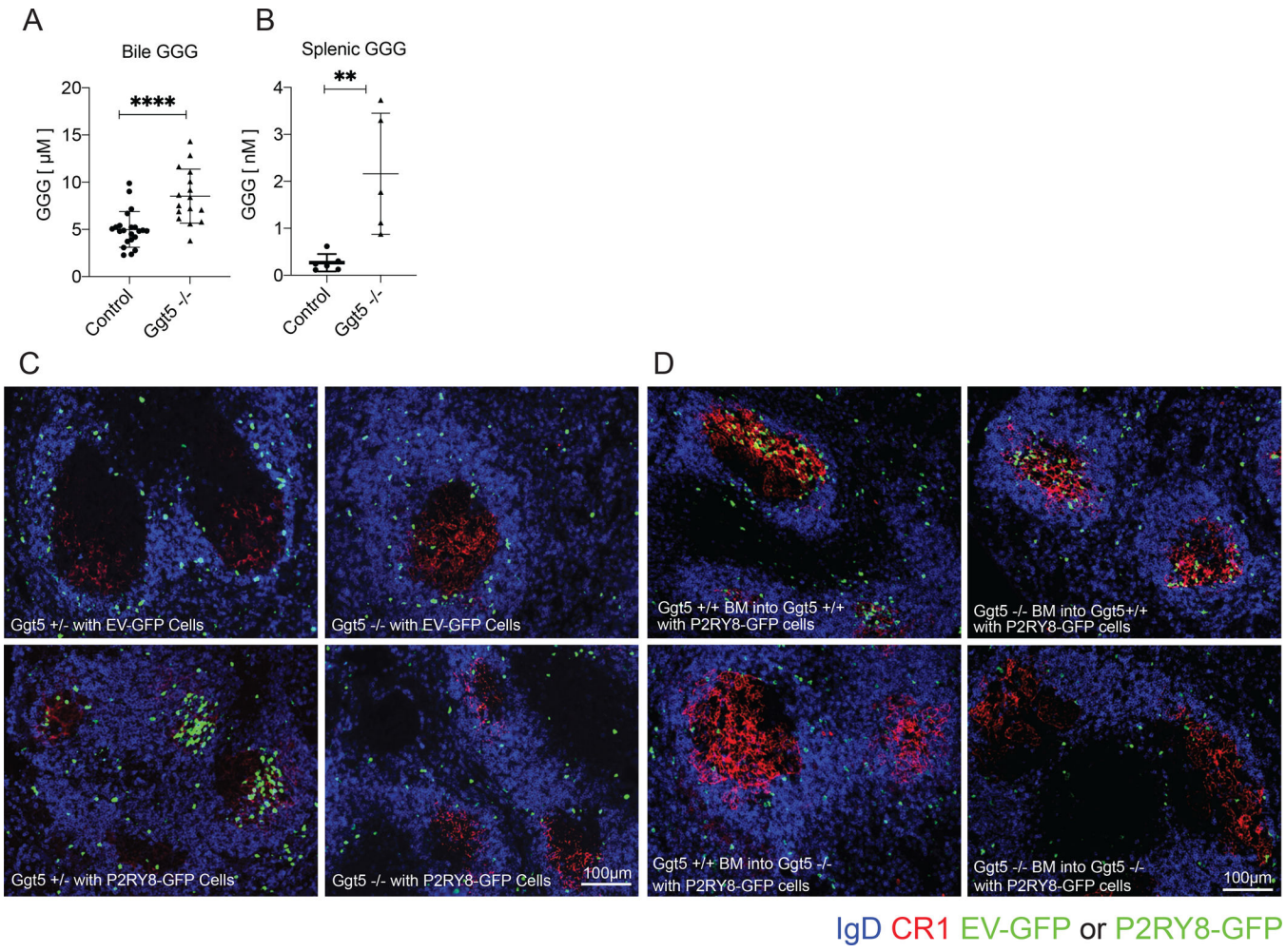

Figure 1: Ggt5 was required for catabolizing tissue GGG and for P2RY8-mediated follicle center confinement of B cells.

(a-b) GGG was measured in the bile (a) and spleen (b) of Ggt5−/− and control (Ggt5+/+ and +/− littermates) by LC-MS/MS. For bile n=22 control and n=16 Ggt5-/−. Spleens were pooled in groups of five (n=6 control, n=5 Ggt5−/−). (c-d) Empty vector (EV) and P2RY8-transduced activated splenic B cells were transferred into preimmunized Ggt5 +/− or −/− mice (c), or Ggt5 BM chimeric mice 8 weeks following reconstitution (d). Immunofluorescence for P2RY8- or EV-transduced B cells (GFP, green) in the splenic GC (CR1, red) of sheep red blood cell (SRBC) immunized mice relative to endogenous follicular B cells (IgD, blue). Scale bars 100µm. Data are pooled from one (a) or three (b) experiments; or representative of six (c) or two (d) biological repeats, with approximately 40 GCs visualized per biological repeat. P-values determined by unpaired two-tailed Student's t-test (a,b) *P<0.05, **P<0.01, ***P<0.001, ****P<0.0001. Graphs depict mean with s.d. and points represent biological replicates.

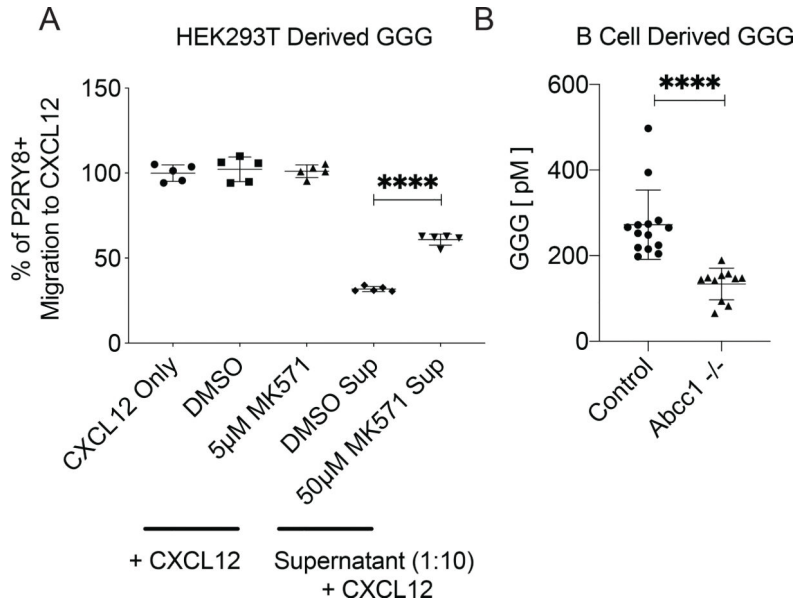

Figure 2: Abcc1 was required for GGG export.

(a) HEK293T cell cultures were treated with 50μM of Abcc1 inhibitor MK571 or the diluted carrier (DMSO) for 16hr. Collected supernatant was used at a 1:10 dilution in a bioassay based on the transwell migration of P2RY8+ WEHI cells towards CXCL12. Control wells contained CXCL12, CXCL12 + DMSO, or CXCL12 + 5μM MK571. (b) Activated, purified splenic B cells from Abcc1−/− and control (Abcc1+/+ and +/− littermate) mice were incubated for 72hrs, after which the supernatant was collected and measured for GGG by LC-MS/MS (n= 14 control, n=11 Abcc1−/−). Data are pooled from (b) or representative of (a) three (b) experiments. P-values determined by unpaired two-tailed Student's t-test (a,b). *P<0.05, **P<0.01, ***P<0.001, ****P<0.0001. Graphs depict mean with s.d. and points represent (a) technical or (b) biological replicates.

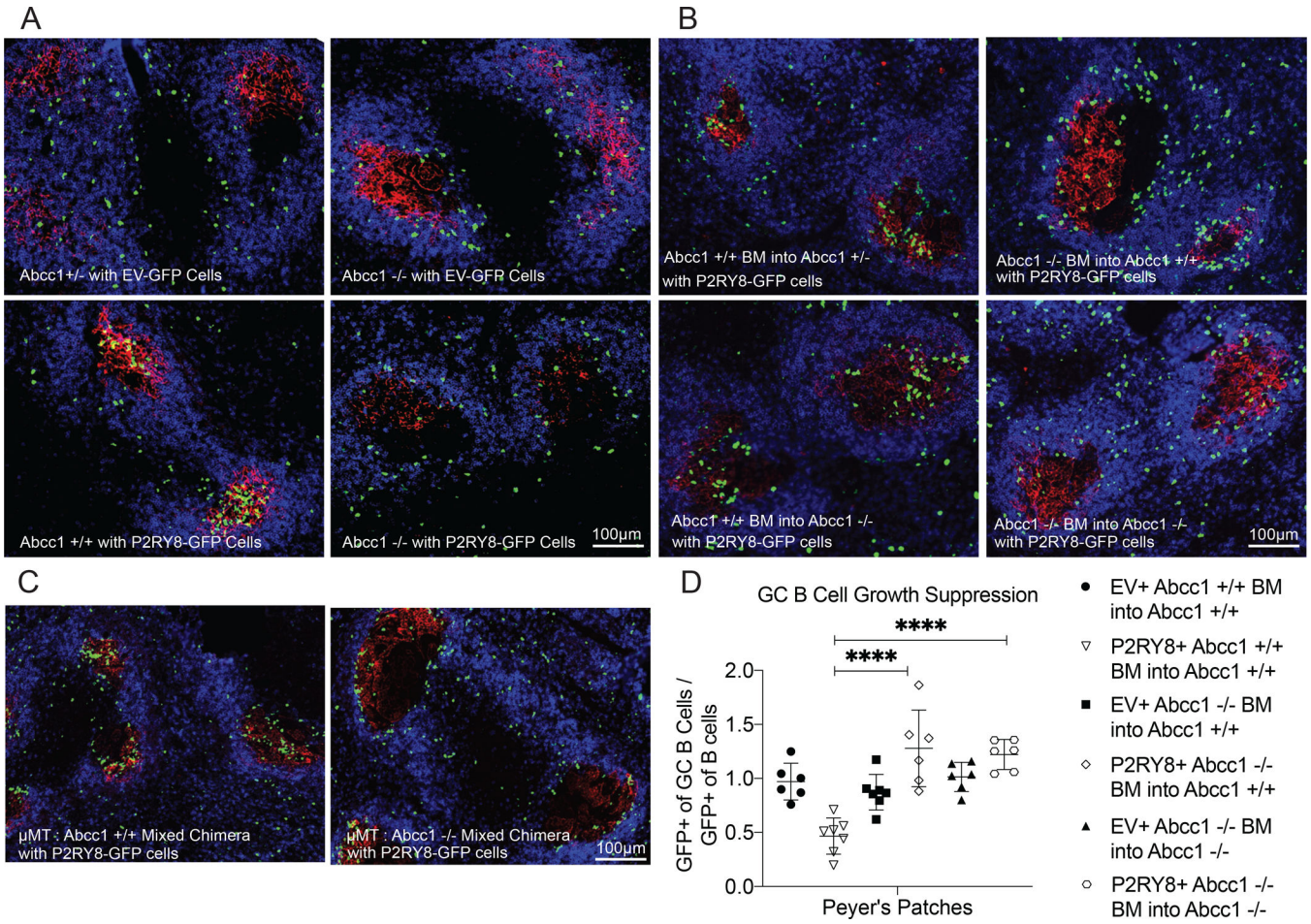

Figure 3: Abcc1 expression by B cells was required for P2RY8-mediated follicle center confinement and for the growth regulation of P2RY8-expressing GC B cells.

(a-c) Activated EV- or P2RY8-transduced polyclonal B cells were transferred into preimmunized Abcc1 +/+, +/− or −/− mice (a), into preimmunized BM chimeric mice of the type indicated (b), or into preimmunized Abcc1+/+ mice reconstituted with μMT BM mixed at a 3:1 ratio with Abcc1+/+ or −/− BM. (c). Immunofluorescence for P2RY8- or EV-transduced B cells (GFP, green) in the GCs (CR1, red) of SRBC immunized mice relative to endogenous follicular B cells (IgD, blue). Scale bars 100μm. (d) Irradiated Abcc1+/+ or −/− mice were reconstituted with P2RY8-GFP or EV-GFP transduced Abcc1+/+ or −/− BM. Following reconstitution, PPs were analyzed for the frequency of GFP+ cells in the follicular and GC B cells compartment. The ratio of GFP+ cells in the GC B cells vs in the follicular B cells was plotted (n=6–7, exact number shown by number of symbols in the plot). Data are pooled from two experiments and representative of four experiments (d); or representative of four (a,b,c) biological repeats, with approximately 40 GCs visualized per biological repeat. P values determined by one-way ANOVA with Tukey's multiple comparisons test (d). *P<0.05, **P<0.01, ***P<0.001, ****P<0.0001. Graphs depict mean with s.d. and points represent biological replicates.

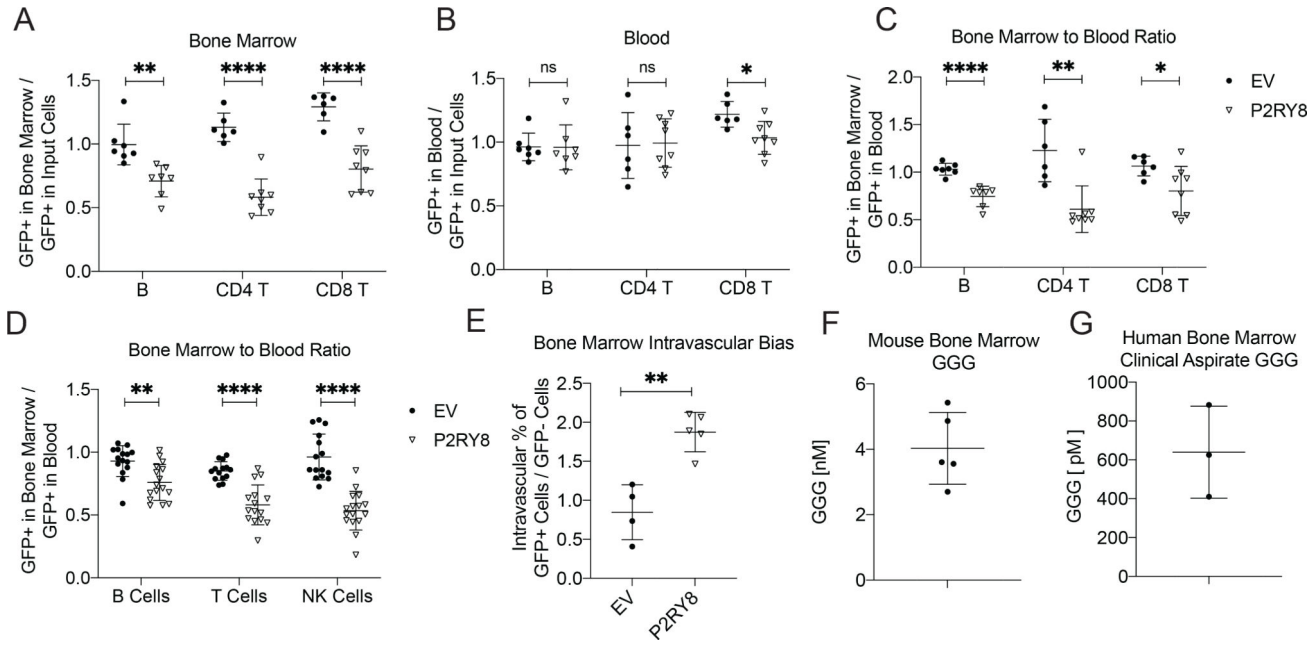

Figure 4: P2RY8 expression reduced lymphocyte homing to the BM.

(a-c,e) Activated EV- or P2RY8-transduced B cells or T cells were transferred into preimmunized mice. GFP+ frequency in the BM (a) or blood (b) after 24hrs is plotted as a ratio of the GFP+ frequency at the time of transfer into mice (input cells). (c) GFP+ frequency in the BM divided by GFP+ frequency in the blood (n=6–8). (d) GFP+ frequency of mature B, T and NK cells in the BM divided by GFP+ frequency in the blood in congenically marked mice reconstituted with EV or P2RY8 transduced BM (n=14–16 per group). (e) Percentage of GFP+ transferred B cells in each mouse staining with CD45.2-PE injected intravascularly, divided by GFP- transferred B cells staining for the same (n=4–5). (f,g) GGG measurement via LC-MS/MS of mouse BM (n=5) (f) or human BM aspirate (n=3) (g). Data are pooled from five (B cells in a-c, e), two (T cells in a-c), three (B and NK cells in d, and g), four (T cells in d) experiments; or representative of three (f) experiments. P values determined by unpaired two-tailed Student's t-test. *P<0.05, **P<0.01, ***P<0.001, ****P<0.0001. Graphs depict mean with s.d. and points represent biological replicates.

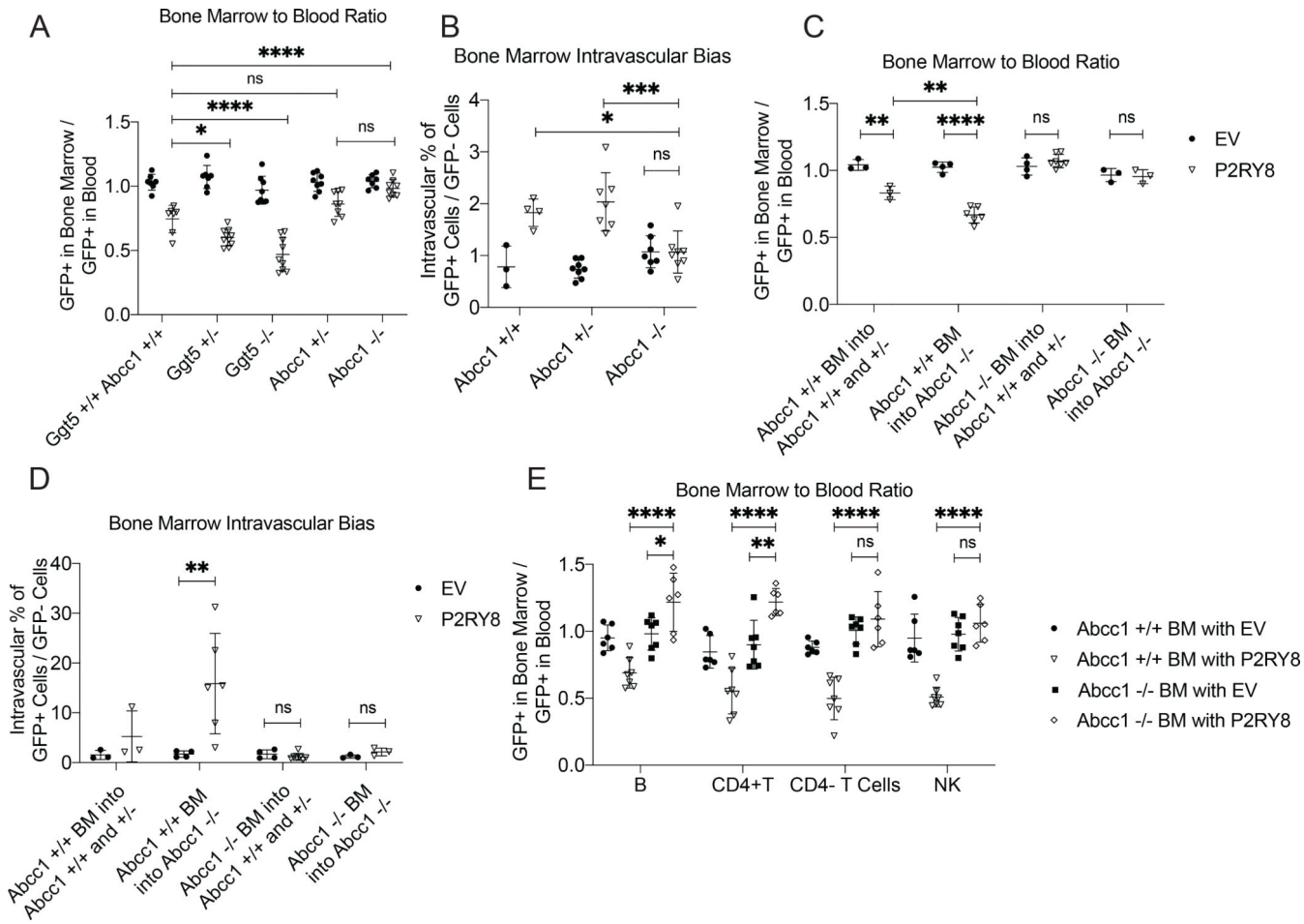

Figure 5: Ggt5 and Abcc1 controlled homing of P2RY8+ lymphocytes to the BM.

(a-d) Activated EV- or P2RY8-transduced polyclonal B cells were transferred into preimmunized mice. (a) GFP+ frequency in the BM divided by GFP+ frequency in the blood at 24hrs after cell transfer (n=7–10 per group). (b) Percentage of GFP+ cells in each mouse staining with CD45.2-PE injected intravascularly, divided by GFP- cell staining for the same (n= 3–10 per group). (c) GFP+ frequency in the BM divided by GFP+ frequency in the blood at 24hrs after cell transfer in Abcc1 chimeric mice. (d) Percentage of GFP+ cells in each individual Abcc1 chimeric mouse staining with CD45.2-PE injected intravascularly, divided by GFP- cell staining for the same (n= 3–7 per group in c,d). (e) GFP+ frequency of mature B, T and NK cells in the BM divided by GFP+ frequency in the blood in congenically marked mice reconstituted with EV- or P2RY8-transduced Abcc1+/+ or −/− BM. Data from Abcc1+/+ BM from this panel is also included in Fig 4d (n=6–7 per group). Data are pooled from seven (a), three (b,c,d), or two (e) experiments. P values determined by one-way ANOVA with Tukey's multiple comparisons test (d). *P<0.05, **P<0.01, ***P<0.001, ****P<0.0001. Graphs depict mean with s.d. and points represent biological replicates.

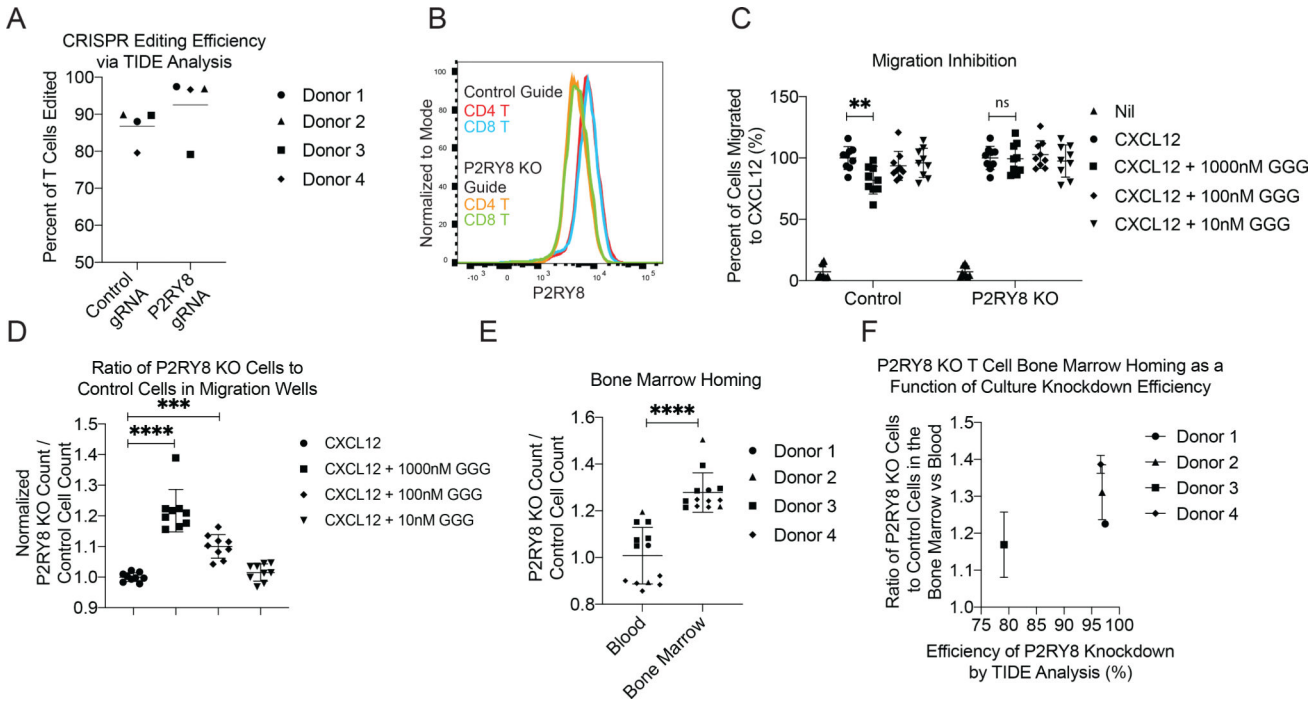

Figure 6: P2RY8 KO Human T cells showed elevated BM homing.

Guide RNAs targeting P2RY8 and the AAVS locus (as a control) were used to edit stimulated primary human T cells from 4 donors. (a) TIDE analysis determined CRISPR editing efficiency for each donor. (b) Staining of CRISPR-edited T cells for P2RY8 protein via flow cytometry. (c-f) P2RY8 KO and AAVS KO control T cells from each donor were CFSE and CTV labeled, respectively, and then mixed at a 1:1 ratio. (c-d) Transwell migration assays of the edited cells towards CXCL12 and the indicated concentrations of GGG. (c) Total counts of P2RY8 KO or AAVS KO control cells found to have migrated to the bottom of each transwell, normalized to the count of migrated cells to CXCL12 alone. (d) Ratio of total P2RY8 KO to AAVS KO controls cells in the bottom of each transwell, normalized to the ratio of migrated cells to CXCL12 alone. (e) A 1:1 mix of CFSE+ P2RY8 KO cells and CTV+ AAVS KO control cells was transferred iv into NSG mice. 48hrs later blood and BM was collected and the ratio of P2RY8 KO to AAVS KO control cells in each tissue was assessed. Based on number of edited T cells available, 20 million cells from each donor were transferred into 1–5 NSG mice. (f) BM to blood ratio plotted as a function of CRISPR editing efficiency of the P2RY8 locus for each donor. Data are pooled from four experiments. P values determined by one-way ANOVA with Tukey's multiple comparisons test (d) or unpaired two-tailed Student's t-test (c) or paired two-tailed Student's t-test (e). *P<0.05, **P<0.01, ***P<0.001, ****P<0.0001. Graphs depict mean with s.d. and points represent biological replicates, except in (c) where points represent pooled technical replicates from 4 human donors.

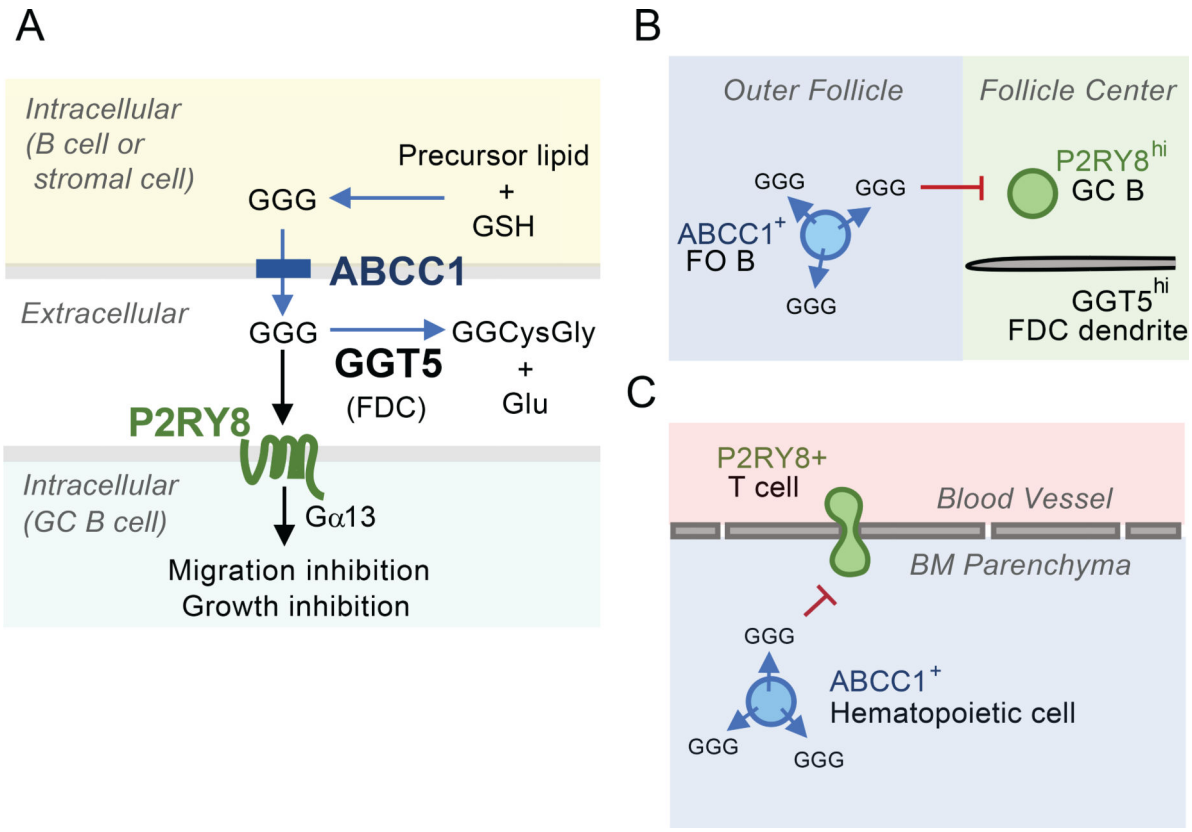

Figure 7: Model figure summarizing ABCC1 and GGT5 function in determining GGG distribution and P2RY8+ cell behavior.

(A) Role of ABCC1 in GGG export from cells, action on P2RY8+ target cells and catabolism in the extracellular space by GGT5. (B) Follicular B cells exporting GGG in an ABCC1-dependent manner and confining P2RY8hi GC B cells to the GGT5hi FDC network at the follicle center. (C) Adherent P2RY8+ T cells in BM blood vessels being have transmigration inhibited (or promoted to undergo reverse transmigration) by GGG produced by ABCC1+ hematopoietic cells in the BM parenchyma.